

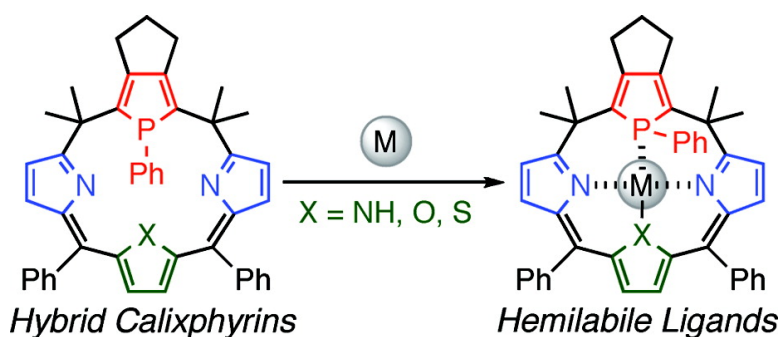
Article

Syntheses, Structures, and Coordination Chemistry of Phosphole-Containing Hybrid Calixphyrins: Promising Macrocyclic P,N,X-Mixed Donor Ligands for Designing Reactive Transition-Metal Complexes

Yoshihiro Matano, Tooru Miyajima, Noriaki Ochi, Takashi Nakabuchi, Motoo Shiro, Yoshihide Nakao, Shigeyoshi Sakaki, and Hiroshi Imahori

J. Am. Chem. Soc., **2008**, 130 (3), 990-1002 • DOI: 10.1021/ja076709o

Downloaded from <http://pubs.acs.org> on February 8, 2009



More About This Article

Additional resources and features associated with this article are available within the HTML version:

- Supporting Information
- Links to the 5 articles that cite this article, as of the time of this article download
- Access to high resolution figures
- Links to articles and content related to this article
- Copyright permission to reproduce figures and/or text from this article

[View the Full Text HTML](#)



ACS Publications
 High quality. High impact.

Syntheses, Structures, and Coordination Chemistry of Phosphole-Containing Hybrid Calixphyrins: Promising Macrocyclic P,N₂,X-Mixed Donor Ligands for Designing Reactive Transition-Metal Complexes

Yoshihiro Matano,^{*,†} Tooru Miyajima,[†] Noriaki Ochi,[†] Takashi Nakabuchi,[†] Motoo Shiro,[‡] Yoshihide Nakao,[†] Shigeyoshi Sakaki,[†] and Hiroshi Imahori^{†,§}

Department of Molecular Engineering, Graduate School of Engineering, Kyoto University, Nishikyo-ku, Kyoto 615-8510, Japan, Rigaku Corporation, Akishima-shi, Tokyo, 196-8666, Japan, and Institute for Integrated Cell-Material Sciences, Kyoto University, Nishikyo-ku, Kyoto 615-8510, Japan

Received September 5, 2007; E-mail: matano@scl.kyoto-u.ac.jp

Abstract: The syntheses, structures, and coordination chemistry of phosphole-containing hybrid calixphyrins (P,N₂,X-hybrid calixphyrins) and the catalytic activities of their transition-metal complexes are reported. The 5,10-porphodimethene type 14- π -P,(NH)₂,X- and 16- π -P,N₂,X-hybrid calixphyrins (X = O, S, NH) are prepared via acid-promoted dehydrative condensation between a σ^4 -phosphatripyrrane and the corresponding 2,5-bis[hydroxy(phenyl)methyl]heteroles followed by DDQ oxidation. Both spectroscopic and crystallographic data of the hybrid calixphyrins have revealed that the conformation and size of the macrocyclic platforms as well as the oxidation state of the π -conjugated pyrrole–heterole–pyrrole (N–X–N) units vary considerably depending on the combination of heteroles. The σ^3 -P,(NH)₂,S- and σ^3 -P,N₂,S-hybrids react with Pd(OAc)₂ and Pd(dba)₂, respectively, to afford the same Pd(II)–P,N₂,S-hybrid complex, in which the calixphyrin platform is regarded as a dianionic ligand. In the complexation with [RhCl(CO)₂]₂ in dichloromethane, the σ^3 -P,N₂,S-hybrid behaves as a neutral ligand to afford an ionic Rh(I)–P,N₂,S-hybrid complex, whereas the σ^3 -P,N₂,NH-hybrid behaves as an anionic ligand to produce Rh(III)–P,N₃-hybrid complexes. In the latter reaction, it is likely that a neutral Rh(I)–P,N₃-hybrid complex, generated as a highly nucleophilic intermediate, undergoes C–Cl bond activation of the solvent. The complexation of AuCl(SMe₂) with the σ^3 -P,N₂,X-hybrids (X = S, NH) leads to the formation of the corresponding Au(I)–monophosphine complexes. The spectral data and crystal structures of these metal complexes exhibit the hemilabile nature of the phosphole-containing hybrid calixphyrin platforms derived from the flexible phosphole unit and the redox active N–X–N units. The hybrid calixphyrin–palladium and –rhodium complexes catalyze the Heck reaction and hydrosilylations, respectively, implying that the metal center in the core is capable of activating the substrates under appropriate reaction conditions. The present results demonstrate the potential utility of the phosphole-containing hybrid calixphyrins as a new class of macrocyclic P,N₂,X-mixed donor ligands for designing highly reactive transition-metal complexes.

Introduction

The development of phosphorus-containing macrocyclic mixed-donor ligands has emerged as an important subject in coordination chemistry, because they provide characteristic chelating sites that are difficult to construct with their acyclic analogues.^{1–6} Such hybrid macrocyclic donors are highly promising for designing reactive and multifunctional transition-

metal catalysts, as (1) the metal center can be supported and stabilized by multidentate platforms, (2) various coordination properties, such as coordination number, cavity size, and σ -donating and π -accepting abilities, are available by changing the components of the heteroatom donors, and (3) conformational mobility of the ligands is controllable by suitable choice

[†] Graduate School of Engineering, Kyoto University.

[‡] Rigaku Corporation.

[§] Institute for Integrated Cell-Material Sciences, Kyoto University.

(1) For reviews, see: (a) McAuliffe, C. A. In *Comprehensive Coordination Chemistry*; Wilkinson, G., Gillard, R. D., McCleverty, J. A., Eds.; Pergamon: Oxford, England, 1987; Vol. 2, pp 995–1004. (b) Stelzer, O.; Langhans, K.-P. In *The Chemistry of Organophosphorus Compounds*; Hartley, F. R., Ed.; Wiley: Chichester, U.K., 1990; Vol. 1, pp 226–233. (c) Caminade, A.-M.; Majoral, J. P. *Chem. Rev.* **1994**, *94*, 1183–1213. (d) Dilworth, J. R.; Wheatley, N. *Coord. Chem. Rev.* **2000**, *199*, 89–158. (e) Mathey, F. *Acc. Chem. Res.* **2004**, *37*, 954–960 and references therein.

(2) (a) Riker-Nappier, J.; Meek, D. W. *J. Chem. Soc., Chem. Commun.* **1974**, 442–443. (b) Scanlon, L. G.; Tsao, Y.-Y.; Cummings, S. C.; Toman, K.; Meek, D. W. *J. Am. Chem. Soc.* **1980**, *102*, 6849–6851. (c) Scanlon, L. G.; Tsao, Y.-Y.; Toman, K.; Cummings, S. C.; Meek, D. W. *Inorg. Chem.* **1982**, *21*, 1215–1221. (3) (a) Kyba, E. P.; Hudson, C. W.; McPhaul, M. J.; John, A. M. *J. Am. Chem. Soc.* **1977**, *99*, 8053–8054. (b) Kyba, E. P.; Chou, S.-S. *P. J. Org. Chem.* **1981**, *46*, 860–863. (c) Kyba, E. P.; Davis, R. E.; Hudson, C. W.; John, A. M.; Brown, S. B.; McPhaul, M. J.; Liu, L.-K.; Glover, A. C. *J. Am. Chem. Soc.* **1981**, *103*, 3868–3875. (d) Kyba, E. P.; Davis, R. E.; Fox, M. A.; Clubb, C. N.; Liu, S.-T.; Reitz, G. A.; Scheuler, V. J.; Kashyap, R. P. *Inorg. Chem.* **1987**, *26*, 1647–1658. (4) Cabral, J. de O.; Cabral, M. F.; Drew, M. G. B.; Nelson, S. M.; Rodgers, A. *Inorg. Chim. Acta* **1977**, *25*, L77–L79.

of the bridging atoms/groups. Despite these promising aspects, however, transition-metal catalysts featuring phosphorus-containing hybrid macrocycles as supporting ligands have not been explored much, owing to limited information on the relationship between their fundamental reactivities and their structural and electronic properties. Accordingly, the search for a new series of hybrid macrocyclic donors is still the subject of growing interest.

Calixphyrins are a class of compounds that include multi-dentate platforms derived from both porphyrins and calixpyrroles and lie at the intersection between these two parent macrocycles.⁷ However, the structural and electronic properties of calixphyrins are unambiguously distinguishable from those of porphyrins and calixpyrroles. Owing to the involvement of both sp^2 - and sp^3 -hybridized bridging meso carbons, calixphyrins possess reasonably flexible frameworks as well as rather rigid π -conjugated networks, whose characters vary considerably depending on the number and position of the sp^3 -meso carbon atoms. Recently, Sessler et al. have established convenient methods for the synthesis of a series of calix[n]phyrins and systematically investigated their structures and conformational mobilities in relation to calix[n]pyrrole chemistry.⁸ Senge et al. have independently developed their own approaches to this class of compounds.⁹ Floriani et al. studied the structures of calix-[4]phyrin-early transition-metal complexes,¹⁰ and some other groups have reported fundamental properties and functionalization of calixphyrins.¹¹ However, the great potential of calixphyrin platforms in transition-metal catalysis has not been addressed so far.

Core-modification is a straightforward approach to add valuable coordinating properties into the porphyrinoid com-

pounds.¹² Indeed, a number of core-modified porphyrins, especially those containing chalcogen or carbon atoms, have been prepared, and their coordination chemistry has been extensively studied. In sharp contrast, no attempt had been made to prepare heteroatom-containing calixphyrins until recently.¹³ We anticipated that replacement of the pyrrole nitrogen atoms of calixphyrin with other heteroatoms, namely replacing the pyrrole ring by other heteroles, would provide new classes of macrocyclic mixed-donor ligands with their coordinating properties such as size, charge, and donating ability, being strongly dependent on the relevant heteroatoms. Phosphole is known as a basically nonaromatic heterole because of insufficient π -conjugation between the cis-dienic π -system and a lone pair of the phosphorus atom.¹⁴ Consequently, phospholes exhibit characteristic-coordinating properties that differ significantly from those of pyrroles and have been utilized as reliable phosphine ligands in transition-metal catalysts.¹⁵ With this in mind, we decided to systematically investigate the coordination chemistry of phosphole-containing hybrid calixphyrins and to shed light on the catalytic activities of their transition-metal complexes.^{16–18}

- (5) (a) Fryzuk, M. D.; Love, J. B.; Rettig, S. J. *Chem. Commun.* **1996**, 2783–2784. (b) Fryzuk, M. D.; Love, J. B.; Rettig, S. J.; Young, V. G. *Science* **1997**, *275*, 1445–1447. (c) Muñoz, J. A.; Escriche, L.; Casabó, J.; Pérez-Jiménez, C.; Kivekäs, R.; Sillanpää, R. *Inorg. Chem.* **1997**, *36*, 947–949. (d) Fryzuk, M. D.; Love, J. B.; Rettig, S. J. *Organometallics* **1998**, *17*, 846–853. (e) Fryzuk, M. D.; Giesbrecht, G. R.; Rettig, S. J. *Inorg. Chem.* **1998**, *37*, 6928–6934. (f) Fryzuk, M. D.; Johnson, S. A.; Rettig, S. J. *Organometallics* **1999**, *18*, 4059–4067. (g) Fryzuk, M. D.; Kozak, C. M.; Bowdridge, M. R.; Jin, W.; Tung, D.; Patrick, B. O.; Rettig, S. J. *Organometallics* **2001**, *20*, 3752–3761. (h) Fryzuk, M. D.; Kozak, C. M.; Mehrkhodavandi, P.; Morello, L.; Patrick, B. O.; Rettig, S. J. *J. Am. Chem. Soc.* **2002**, *124*, 516–517. (i) Fryzuk, M. D.; Kozak, C. M.; Bowdridge, M. R.; Patrick, B. O.; Rettig, S. J. *J. Am. Chem. Soc.* **2002**, *124*, 8389–8397. (j) Fryzuk, M. D.; Kozak, C. M.; Bowdridge, M. R.; Patrick, B. O. *Organometallics* **2002**, *21*, 5047–5054.
- (6) (a) Muñoz, J. A.; Escriche, L.; Casabó, J.; Pérez-Jiménez, C.; Kivekäs, R.; Sillanpää, R. *Inorg. Chem.* **1997**, *36*, 947–949. (b) Escriche, L.; Muñoz, J. A.; Rosell, J.; Kivekäs, R.; Sillanpää, R.; Casabó, J. *Inorg. Chem.* **1998**, *37*, 4807–4813.
- (7) The term *calixphyrin* was proposed by Sessler and co-workers to describe the family of porphomethene, porphodimethene, porphotrimethene, and their expanded analogues in a generic sense. Král, V.; Sessler, J. L.; Zimmerman, R. S.; Seidel, D.; Lynch, V.; Andrioletti, B. *Angew. Chem., Int. Ed.* **2000**, *39*, 1055–1058.
- (8) (a) Bucher, C.; Seidel, D.; Lynch, V.; Král, V.; Sessler, J. L. *Org. Lett.* **2000**, *2*, 3103–3106. (b) Bucher, C.; Zimmerman, R. S.; Lynch, V.; Král, V.; Sessler, J. L. *J. Am. Chem. Soc.* **2001**, *123*, 2099–2100; correction, 12744. (c) Sessler, J. L.; Zimmerman, R. S.; Bucher, C.; Král, V.; Andrioletti, B. *Pure Appl. Chem.* **2001**, *73*, 1041–1057. (d) Dolensky, B.; Kroulík, J.; Král, V.; Sessler, J. L.; Dvoráková, H.; Bour, P.; Bernátková, M.; Bucher, C.; Lynch, V. *J. Am. Chem. Soc.* **2004**, *126*, 13714–13722.
- (9) (a) Senge, M. O.; Kalisch, W. W.; Bischoff, I. *Chem. Eur. J.* **2000**, *6*, 2721–2738. (b) Senge, M. O. *Acc. Chem. Res.* **2005**, *38*, 733–743. (c) Sergeeva, N. N.; Senge, M. O. *Tetrahedron Lett.* **2006**, *47*, 6169–6172.
- (10) (a) Benech, J.-M.; Bonomo, L.; Solari, E.; Scopelliti, R.; Floriani, C. *Angew. Chem., Int. Ed.* **1999**, *38*, 1957–1959. (b) Bonomo, L.; Toraman, G.; Solari, E.; Scopelliti, R.; Floriani, C. *Organometallics* **1999**, *18*, 5198–5200.
- (11) For example, see: (a) Krattinger, B.; Callot, H. J. *Tetrahedron Lett.* **1998**, *39*, 1165–1168. (b) Harmjanz, M.; Gill, H. S.; Scott, M. J. *J. Org. Chem.* **2001**, *66*, 5374–5383. (c) Bernátková, M.; Andrioletti, B.; Král, V.; Rose, E.; Vaissermann, J. *J. Org. Chem.* **2004**, *69*, 8140–8143. (d) Bucher, C.; Devillers, C. H.; Moutet, J.-C.; Pécaut, J.; Royal, G.; Saint-Aman, E.; Thomas, F. *Dalton Trans.* **2005**, 3620–3631. (e) O'Brien, A. Y.; McGann, J. P.; Geier, G. R., III. *J. Org. Chem.* **2007**, *72*, 4084–4092.
- (12) (a) Latos-Grażyński, L. In *The Porphyrin Handbook*; Kadish, K. M., Smith, K. M., Guillard, R., Eds.; Academic Press: San Diego, CA, 2000; Vol. 2, Chapter 14. (b) Chandrashekar, T. K.; Venkatraman, S. *Acc. Chem. Res.* **2003**, *36*, 676–691. (c) Sessler, J. L.; Seidel, D. *Angew. Chem., Int. Ed.* **2003**, *42*, 5134–5175. (d) Furuta, H.; Maeda, H.; Osuka, A. *Chem. Commun.* **2002**, 1795–1804. (e) Srinivasan, A.; Furuta, H. *Acc. Chem. Res.* **2005**, *38*, 10–20. (f) Chmielewski, P. J.; Latos-Grażyński, L. *Coord. Chem. Rev.* **2005**, *249*, 2510–2533. (g) Stepien, M.; Latos-Grażyński, L. *Acc. Chem. Res.* **2005**, *38*, 88–98. (h) Gupta, I.; Ravikanth, M. *Coord. Chem. Rev.* **2006**, *250*, 468–518. (i) Pawlicki, M.; Latos-Grażyński, L. *Chem. Rec.* **2006**, *6*, 64–78 and references therein.
- (13) Recently, the synthesis and structures of sulfur-containing phlorins were reported. Gupta, I.; Fröhlich, R.; Ravikanth, M. *Chem. Commun.* **2006**, 3726–3728.
- (14) (a) Quin, L. D. *The Heterocyclic Chemistry of Phosphorus*; Wiley: New York, 1981. (b) Mathey, F. *Chem. Rev.* **1988**, *88*, 429–453. (c) Quin, L. D. In *Comprehensive Heterocyclic Chemistry*; Katritzky, A. R., Rees, C. W., Scriven, E. F. V., Eds.; Elsevier: Oxford, 1996; Vol. 2. (d) Mathey, F.; Mercier, F. C. R. *Acad. Sci. Paris, Sér. II b* **1997**, 701–716. (e) Hay, C.; Hissler, M.; Fischmeister, C.; Rault-Berthelot, J.; Toupet, L.; Nyulászi, L.; Réau, R. *Chem. Eur. J.* **2001**, *7*, 4222–4236. (f) Delaere, D.; Nguyen, M. T.; Vanquickenborne, L. G. *Phys. Chem. Chem. Phys.* **2002**, *4*, 1522–1530. (g) Delaere, D.; Nguyen, M. T.; Vanquickenborne, L. G. *J. Phys. Chem. A* **2003**, *107*, 838–846. (h) Hissler, M.; Dyer, P. W.; Réau, R. *Coord. Chem. Rev.* **2003**, *244*, 1–44. (i) Mathey, F. *Angew. Chem., Int. Ed.* **2003**, *42*, 1578–1604. (j) Baumgartner, T.; Réau, R. *Chem. Rev.* **2006**, *106*, 4681–4727 and references therein; correction, **2007**, *107*, 303.
- (15) For example, see: (a) Wilkes, L. M.; Nelson, J. H.; McCusker, L. B.; Seff, K.; Mathey, F. *Inorg. Chem.* **1983**, *22*, 2476–2485. (b) Choudary, B. M.; Reddy, N. P.; Jamil, M. Z. *Polyhedron* **1986**, *5*, 911–912. (c) Neibecker, D.; Réau, R. *J. Mol. Catal.* **1989**, *57*, 153–163. (d) Neibecker, D.; Réau, R. *J. Mol. Catal.* **1989**, *53*, 219–227. (e) Doherty, S.; Robins, E. G.; Knight, J. G.; Newman, C. R.; Rhodes, B.; Champkin, P. A.; Clegg, W. J. *Organomet. Chem.* **2001**, *640*, 182–196. (f) Sauthier, M.; Leca, F.; Toupet, L.; Réau, R. *Organometallics* **2002**, *21*, 1591–1602. (g) Bergounhou, C.; Neibecker, D.; Mathieu, R. *Organometallics* **2003**, *22*, 782–786. (h) Thoumazet, C.; Melaimi, M.; Ricard, L.; Le Floch, P. C. R. *Acad. Sci., Ser. IIc: Chim.* **2004**, *7*, 823–832. (i) Melaimi, M.; Thoumazet, C.; Ricard, L.; Le Floch, P. J. *Organomet. Chem.* **2004**, *689*, 2988–2994. (j) Mora, G.; van Zutphen, S.; Thoumazet, C.; Le Goff, X. F.; Ricard, L.; Grutzmacher, H.; Le Floch, P. *Organometallics* **2006**, *25*, 5528–5532. (k) Thoumazet, C.; Grutzmacher, H.; Deschamps, B.; Ricard, L.; Le Floch, P. *Eur. J. Inorg. Chem.* **2006**, 3911–3922. (l) Mora, G.; Deschamps, B.; van Zutphen, S.; Le Goff, X. F.; Ricard, L.; Le Floch, P. *Organometallics* **2007**, *26*, 1846–1855.
- (16) For the chemistry of phosphole-containing macrocycles, see: (a) Mathey, F.; Mercier, F.; Nief, F.; Fischer, J.; Mitschler, A. *J. Am. Chem. Soc.* **1982**, *104*, 2077–2079. (b) Beviere, M.-O.; Mercier, F.; Ricard, L.; Mathey, F. *Angew. Chem., Int. Ed.* **1990**, *29*, 655–657. (c) Laporte, F.; Mercier, F.; Ricard, L.; Mathey, F. *J. Am. Chem. Soc.* **1994**, *116*, 3306–3311. (d) Deschamps, E.; Ricard, L.; Mathey, F. *J. Chem. Soc., Chem. Commun.* **1995**, 1561. (e) Mercier, F.; Laporte, F.; Ricard, L.; Mathey, F.; Schröder, M.; Regitz, M. *Angew. Chem., Int. Ed. Engl.* **1997**, *36*, 2364–2366. (f) Robé, E.; Ortega, C.; Mikina, M.; Mikolajczyk, M.; Daran, J.-C.; Gouygou, M. *Organometallics* **2005**, *24*, 5549–5559.
- (17) Recently, we reported the first examples of phosphole-containing hybrid calixpyrroles. Matano, Y.; Nakabuchi, T.; Miyajima, T.; Imahori, H. *Organometallics* **2006**, *25*, 3105–3107.

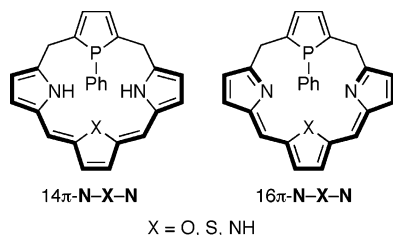


Figure 1. Macrocyclic skeletons of phosphole-containing hybrid calixphyrins.

Figure 1 illustrates the macrocyclic skeletons of our target molecules, 5,10-porphodimethene-type¹⁹ phosphole-containing hybrid calixphyrins, which are designed to provide different chelating modes derived from the heterole subunits combined. That is, the hybrid ligands in Figure 1 contain a flexible phosphole unit connected through the sp^3 -meso bridges and the π -conjugated pyrrole–heterole–pyrrole (N–X–N) unit linked by the sp^2 -meso carbons. These structural properties are beneficial for the construction of new reactive transition metal catalysts. Thus, a flipping motion occurring at the phosphole part would generate a coordinatively unsaturated metal center, which can be indispensable for activating substrates. Furthermore, changing the combination of heterole rings at the N–X–N unit adds diverse electronic properties at the π -conjugated backbone. Additionally, two possible π -networks, 14π -N–X–N and 16π -N–X–N, are conceivable, and, as a consequence, four charge distributions from zero to -3 are attainable for X = O, S, NH at least in a formal sense.

Here, we report the first comprehensive study on the syntheses, structures, and coordinating properties of a series of phosphole-containing hybrid calixphyrins of the 5,10-porphodimethene-P,(NH)₂,X- and P,N₂,X-types (X = O, S, NH).²⁰ It has been revealed that the electronic nature of the central heterole X strongly affects the π -conjugated structure of the N–X–N unit (X = furan, thiophene, and pyrrole) in the calixphyrin platforms. In the complexation with palladium, rhodium, and gold, the hybrid calixphyrins exhibit diverse coordination behavior derived from the flexible phosphole unit and the redox active N–X–N unit. Thus, the oxidation state, charge, and coordination number at the metal center, which have been fully characterized by NMR spectroscopy, X-ray crystallography, and theoretical calculations, are deeply related to the combination with the heterole ligands. Moreover, the Pd–P,N₂,X- and Rh–P,N₂,X-hybrid complexes have proven to catalyze the Heck reaction and hydrosilylations, respectively, under appropriate reaction conditions, demonstrating that the phosphole-containing hybrid calixphyrins behave as hemilabile and redox-active ligands.²¹ It is of utmost interest that reciprocal electronic communication between the metal and the N–X–N unit plays a crucial role in the bond-activation processes by these M–P,N₂,X-hybrid complexes.

Results and Discussion

I. Syntheses of Phosphole-Containing Hybrid Calixphyrins. Phosphole-containing hybrid calixphyrins **3–6** were synthesized starting from σ^4 -phosphatripyrrane **1**¹⁷ and the corresponding 2,5-difunctionalized heteroles **2**, as shown in Scheme 1. Treatment of a CH₂Cl₂ solution containing **1** and 2,5-bis[hydroxy(phenyl)methyl]thiophene (**2S**)²² with BF₃·OEt₂ at room-temperature gave a mixture of condensation products, which was then reacted with 2.2 equiv of 2,3-dichloro-5,6-dicyanobenzoquinone (DDQ) to afford the σ^4 -P,(NH)₂,S-hybrid calixphyrin **3S** and the σ^4 -P,N₂,S-hybrid calixphyrin **4S** in 5% and 24% yield, respectively. These two products were easily separated by silica gel column chromatography. On the basis of the oxidation state of the π -conjugated part, **3S** is classified as the 2e-oxidized product and **4S** as the 4e-oxidized product. That is, **3S** contains the 14π -conjugated N–S–N unit, whereas **4S** contains the 16π -N–S–N unit. It was independently confirmed that **3S** can be converted to **4S** in good yield by treatment with excess DDQ. When 2,5-bis[hydroxy(phenyl)methyl]furan (**2O**)²³ and 2,5-bis[hydroxy(phenyl)methyl]pyrrole (**2N**)²⁴ were used in place of **2S**, the σ^4 -P,(NH)₂,O-hybrid **3O** and the σ^4 -P,N₂,NH-hybrid **4N** were isolated in 19% and 30% yield, respectively. The 14π -N–O–N unit in the 2e-oxidized product **3O** could not be further oxidized even in the presence of excess DDQ, whereas no 2e-oxidized product was obtained in the synthesis of **4N**.

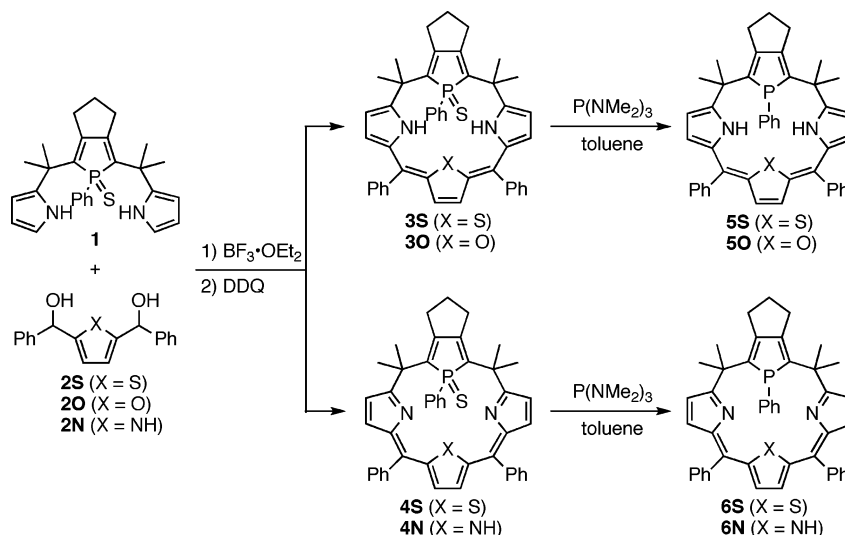
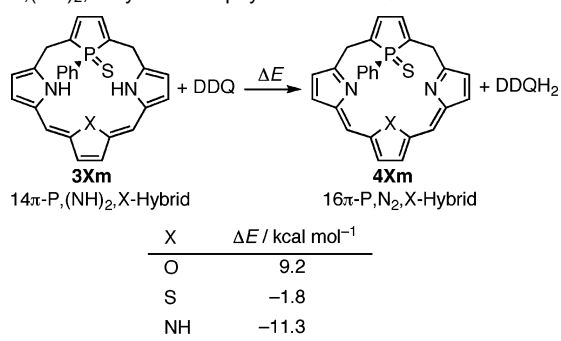
When heated with excess P(NMe₂)₃ in refluxing toluene, the σ^4 -P,N₂,S-hybrid **4S** was converted to the σ^3 -P,N₂,S-hybrid **6S** in 87% yield. Similarly, the σ^4 -phosphorus center in **3O**, **3S**, and **4N** was reduced efficiently by P(NMe₂)₃, affording the σ^3 -P,(NH)₂,O-hybrid **5O**, the σ^3 -P,(NH)₂,S-hybrid **5S**, and the σ^3 -P,N₂,NH-hybrid **6N**, respectively, in 81–92% yields.

The above results indicate that the redox properties of the π -conjugated N–X–N units in the hybrid calixphyrins are definitely dependent on the nature of the central heteroles. To know the intrinsic factors determining the $14\pi/16\pi$ (**3X/4X**) selectivity, we evaluated the reaction energies of the DDQ oxidation of 14π -P,(NH)₂,X-hybrid calixphyrin models **3Xm** to the corresponding 16π -P,N₂,X-hybrid calixphyrin models **4Xm** on the basis of density functional theory (DFT) calculations. The optimized structures are depicted in Figures S1 and S2 together with selected bond parameters. Further computational details are summarized in the Experimental Section.

As shown in Scheme 2, the oxidation of **3Om** with DDQ is a thermodynamically unfavorable process, as indicated by a large positive reaction energy of 9.2 kcal mol⁻¹. In sharp contrast, the formation of **4Nm** from **3Nm** with DDQ yields a large negative reaction energy of -11.3 kcal mol⁻¹, suggesting that oxidation of the N–N–N unit is thermodynamically favorable. The reaction energy from **3Sm/DDQ** to **4Sm/DDQH₂** is slightly negative (-1.8 kcal mol⁻¹), which indicates that both the 14π

(18) Phosphole-containing porphyrins and a P-confused carborporphyrinoid were reported recently. (a) Delaere, D.; Nguyen, M. T. *Chem. Phys. Lett.* **2003**, *376*, 329–337. (b) Matano, Y.; Nakabuchi, T.; Miyajima, T.; Imahori, H.; Nakano, H. *Org. Lett.* **2006**, *8*, 5713–5716. (c) Duan, Z.; Clochard, M.; Donnadiou, B.; Mathey, F.; Tham, F. S. *Organometallics* **2007**, *26*, 3617–3620.
 (19) Based on the number and position of the sp^3 -carbons, calix[4]phyrins are divided into four classes: porphomethenes, 5,10-porphodimethenes, 5,15-porphodimethenes, and porphotrimethenes.
 (20) For a preliminary result on the P,(NH)₂,S- and P,N₂,S-hybrid calixphyrins, see: Matano, Y.; Miyajima, T.; Nakabuchi, T.; Imahori, H.; Ochi, N.; Sakaki, S. *J. Am. Chem. Soc.* **2006**, *128*, 11760–11761.

(21) For the transition-metal coordination chemistry of hemilabile ligands, see: (a) Jeffrey, J. C.; Rauchfuss, T. B. *Inorg. Chem.* **1979**, *18*, 2658–2666. (b) Allgeier, A. M.; Mirkin, C. A. *Angew. Chem., Int. Ed.* **1998**, *37*, 894–908. (c) Slone, C. S.; Weinberger, D. A.; Mirkin, C. A. In *Progress in Inorganic Chemistry*; Karlin, K. D., Ed.; Wiley: New York, 1999; Vol. 48, pp 233–350. (d) Braunstein, P.; Naud, F. *Angew. Chem., Int. Ed.* **2001**, *40*, 680–699. (e) Weng, Z.; Teo, S.; Hor, T. S. A. *Acc. Chem. Res.* **2007**, *40*, 676–684 and references therein.
 (22) Ulman, A.; Manassen, J. *J. Am. Chem. Soc.* **1975**, *97*, 6540–6544.
 (23) Chmielewski, P. J.; Latos-Grażyński, L.; Olmstead, M. M.; Balch, A. L. *Chem. Eur. J.* **1997**, *3*, 268–278.
 (24) Heo, P.-Y.; Lee, C.-H. *Bull. Korean Chem. Soc.* **1996**, *17*, 515–520.

Scheme 1. Synthesis of Phosphole-Containing Hybrid Calixphyrins 3–6**Scheme 2.** Reaction Energies Calculated for Oxidation of 14 π -P,(NH)₂,X-Hybrid Calixphyrins with DDQ^a

^a DDQ = 2,3-dichloro-5,6-dicyanobenzoquinone; DDQH₂ = 2,3-dichloro-5,6-dicyanoquinone.

and 16 π systems are isolable. These theoretical results are in good agreement with the experimental results qualitatively. The differences in reaction energies among X = O, S, and NH are reasonably interpreted in terms of the electrostatic interaction of the NH groups with X in 3Xm and the interaction of the N lone pairs with X in 4Xm.^{25,26}

II. Characterization of Phosphole-Containing Hybrid Calixphyrins. The hybrid calixphyrins 3–6 were fully characterized by conventional spectroscopic techniques (¹H, ¹³C, and ³¹P NMR and HRMS). Representative spectral features of 5X (X = O, S) and 6X (X = S, N) are as follows. The ³¹P chemical shifts of 5S (δ 31.0 ppm) and 6S (δ 26.7 ppm) are close to those of 5O (δ 32.6 ppm) and 6N (δ 24.0 ppm), respectively, suggesting that changing the combination of heterole subunits

at the N–X–N part does not significantly affect the electronic character of the phosphorus nuclei in the phosphole ring. In the ¹H NMR spectra (in CDCl₃) of 5O and 5S, the β protons of the conjugated heterole rings appeared at δ 5.49–6.02 ppm (pyrrole- β of 5O and 5S), δ 5.83 ppm (furan- β of 5O), and δ 6.41 ppm (thiophene- β of 5S). On the other hand, the heterole ring β protons of 6S and 6N were observed at δ 6.56–6.64 ppm (2-azafluvene- β of 6S and 6N), δ 6.60 ppm (thiophene- β of 6S), and δ 5.92 ppm (pyrrole- β of 6N). The difference in chemical shifts of the heterole β protons between the two series of hybrids 5X and 6X reflects the difference in degree of π -conjugation between the 14 π -N–X–N units and the 16 π -N–X–N units. The pyrrole NH protons of 5O, 5S, and 6N appeared at δ 8.94, 8.68, and 11.36 ppm, respectively.

The structures of 5O, 6S, and 6N were further elucidated by X-ray crystallography. The ORTEP diagrams are shown in Figures 2–4, the crystallographic parameters are summarized in Table S1, and selected distances, bond lengths, and dihedral angles are listed in Table 1. The 14 π - σ^3 -P,(NH)₂,O-hybrid 5O is largely twisted at the N–O–N unit with dihedral angles between the pyrrole and furan ring planes of 26.9–29.4°. The equivalent appearance of the pyrrole- β protons of 5O in its ¹H NMR spectrum (vide supra) suggests that the N–O–N unit is fluxional in solution. By contrast, the σ^3 -P,N₂,S-hybrid 6S and the σ^3 -P,N₂,NH-hybrid 6N are composed of almost flat 16 π -N–X–N planes (X = S, N) with small dihedral angles of 1.9–10.1°. The observed conformation of 6N differs considerably from those of the 5,10-porphodimethene-type calix[4]phyrins reported earlier, which exhibit a nonplanar, twisted conformation.^{8a,11a} This is attributable to the difference in size of the macrocyclic platform; the present phosphole-containing hybrid calixphyrin 6N is apparently larger than that of the parent calix[4]phyrin. In the hybrids 6S and 6N, the phosphole ring stands almost perpendicular to a mean plane formed by the four meso carbon atoms with dihedral angles of 85.1° and 85.9°, respectively.

The 14 π -conjugated structure of the N–O–N unit and the 16 π -conjugated structures of the N–S–N and N–N–N units are clearly reflected in the carbon–carbon/nitrogen bond alternation at the heterole rings and the inter-ring bridges (abbreviated as *d–l* in Table 1). It is known that the geometrical aromaticity of the pyrrole ring is larger than that of the

(25) In the case of X = O, stabilization attained by the π -extension of the N–O–N unit from 14 π to 16 π does not compensate for the large destabilization caused by the loss of the attractive hydrogen-bonding interaction in 3Om and the gain of the repulsive interaction among the lone pairs at the core in 4Om. In the case of X = NH, the highly strained conformation owing to the repulsive interaction among the NH groups in 3Nm is relaxed by dehydrogenative oxidation, and the attractive hydrogen-bonding interaction arises between the lone pairs and the NH group in 4Nm. Totally, a large stabilization is gained by the π -extension of the N–N–N unit from 14 π to 16 π . In the case of X = S, the loss of attractive interaction in 3Sm and the gain of repulsive interaction in 4Sm would be smaller as compared to those for the furan analogues.

(26) The calculated relative stabilities may also be concerned with the oxidation potentials of pyrrole, thiophene, and furan, which were reported to be +0.8, +1.6, and +1.85 V, respectively (vs. SCE). See: Tourillon, G.; Garnier, F. J. *Electroanal. Chem.* **1982**, *135*, 173–178.

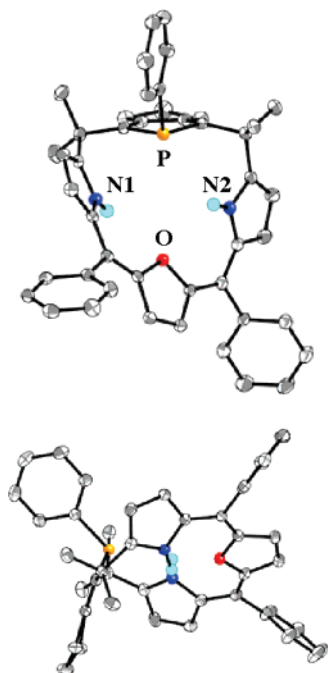


Figure 2. Top and side views of **50** (50% probability ellipsoids). Hydrogen atoms (except for NH) and solvents are omitted for clarity: gray (C), blue (N), red (O), orange (P), sky blue (H). $\Sigma_{C-P-C} = 303.5^\circ$.

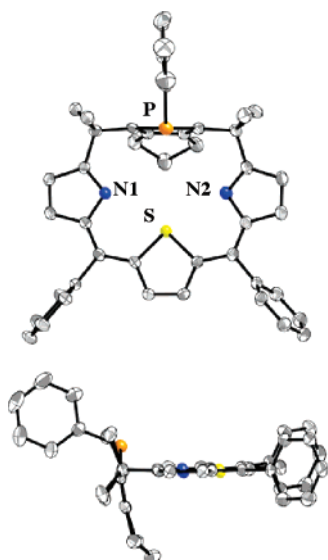


Figure 3. Top and side views of **6S** (one of the pairing molecules; 50% probability ellipsoids). Hydrogen atoms and solvents are omitted for clarity: gray (C), blue (N), orange (P), yellow (S). $\Sigma_{C-P-C} = 302.2^\circ$ and 302.8° .

2-azafulvene (2-methylene-2H-pyrrole) ring.²⁷ Hence, the bond alternation of the pyrrole ring is less significant as compared to that of the 2-azafulvene ring. In **50**, the bond lengths (L) at $d-h$ differ only slightly ($\Delta L = 0.03 \text{ \AA}$), whereas the bond lengths at i and k are longer by $0.07-0.11 \text{ \AA}$ than those at j and l . In **6S** and **6N**, the reverse bond alternation is observed. Thus, the bond lengths at d, f , and i are appreciably shorter than the adjacent bond lengths at e, g , and j ($\Delta L = 0.08-0.17 \text{ \AA}$ for **6S**; $\Delta L = 0.05-0.15 \text{ \AA}$ for **6N**). These data are in good accordance with the canonical structures of **50**, **6S**, and **6N**

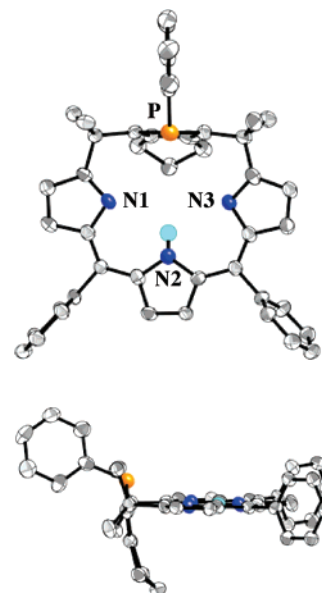


Figure 4. Top and side views of **6N** (one of the pairing molecules; 30% probability ellipsoids). Hydrogen atoms (except for NH) and solvents are omitted for clarity: gray (C), blue (N), orange (P), sky blue (H). $\Sigma_{C-P-C} = 303.3^\circ$ and 305.1° .

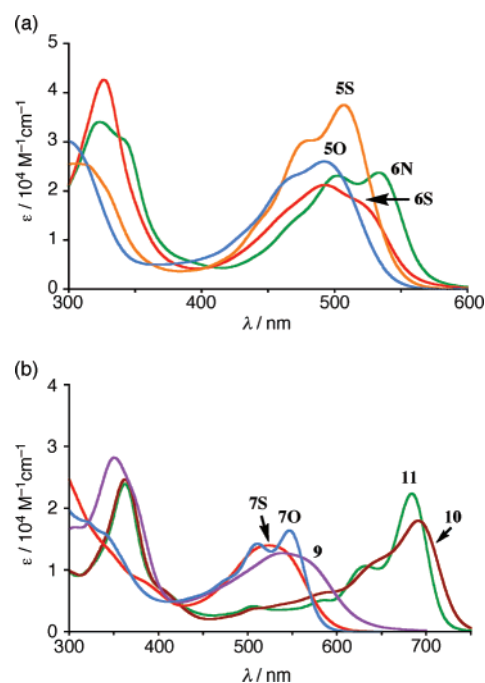
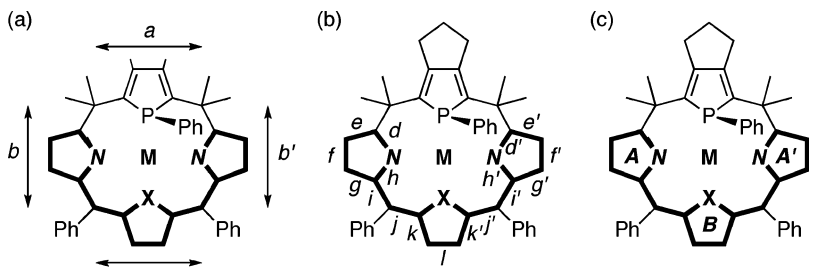


Figure 5. UV-vis absorption spectra of phosphole-containing hybrid calixphyrins and their metal complexes. (a) blue, **5O**; orange, **5S**; red, **6S**; green, **6N**. (b) blue, **7O**; red, **7S**; purple, **9**; brown, **10**; green, **11**.

illustrated in Scheme 1. The meso-meso distance at the N-X-N unit (abbreviated as c ; 5.33 \AA) and the N...N distance (4.82 \AA) of **6S** are longer than the respective distances of **6N** ($4.99-5.04$ and $4.52-4.54 \text{ \AA}$), reflecting the difference in sizes between thiophene and pyrrole rings. Although the sizes of pyrrole and furan are comparable, the meso-meso distance c of **50** is shorter by $0.16-0.21 \text{ \AA}$ than that of **6N**, because of the highly twisted conformation at the N-O-N unit in **50**. For all hybrid calixphyrins characterized, the P -phenyl group is located outside the macrocycle, probably due to steric reasons. As a consequence, the lone pair of the phosphorus atom is

(27) Cyrański, M. K.; Krygowski, T. M.; Wisiorowski, M.; van Eikema Hommes, N. J. R.; Schleyer, P. von R. *Angew. Chem., Int. Ed.* **1998**, *37*, 177-180.

Table 1. Selected Distances, Bond Lengths, and Dihedral Angles of Hybrid Calixpyrins


hybrid	50	6S ^a	6N ^a	70	7S	10 ^b	11 ^c	13S ^d
M, N, X	-, NH, O	-, N, S	-, N, NH	Pd, N, O	Pd, N, S	Rh, N, N	Rh, N, N	Au, N, S
(a) Meso–Meso Distances (Å)								
<i>a</i>	5.53	5.60 (5.60)	5.56 (5.55)	5.48	5.47	5.49	5.48	5.64
<i>b</i>	5.02	4.88 (4.88)	4.93 (4.93)	5.00	5.06	4.99	4.98	4.87
<i>b'</i>	5.02	4.87 (4.88)	4.93 (4.92)	5.08	5.07	5.00	5.03	4.82
<i>c</i>	4.83	5.33 (5.33)	5.04 (4.99)	4.80	5.02	4.88	4.87	5.32
(b) Bond Lengths and Distances (Å) ^e								
<i>d, d'</i>	1.38	1.31 (1.30)	1.33 (1.33)	1.39	1.38	1.34	1.35	1.31
<i>e, e'</i>	1.38	1.46 (1.47)	1.47 (1.48)	1.39	1.39	1.43	1.43	1.46
<i>f, f'</i>	1.41	1.35 (1.34)	1.36 (1.36)	1.40	1.39	1.36	1.36	1.35
<i>g, g'</i>	1.38	1.45 (1.46)	1.46 (1.46)	1.39	1.39	1.42	1.43	1.45
<i>h, h'</i>	1.38	1.42 (1.41)	1.41 (1.42)	1.40	1.41	1.42	1.42	1.41
<i>i, i'</i>	1.45	1.37 (1.36)	1.37 (1.37)	1.45	1.45	1.37	1.38	1.36
<i>j, j'</i>	1.36	1.45 (1.45)	1.44 (1.42)	1.35	1.36	1.43	1.40	1.45
<i>k, k'</i>	1.43	1.38 (1.38)	1.41 (1.41)	1.43	1.45	1.42	1.43	1.38
<i>l</i>	1.34	1.40 (1.40)	1.37 (1.36)	1.35	1.35	1.36	1.36	1.40
N...N	4.59	4.82 (4.82)	4.52 (4.54)	4.08	4.15	4.16	4.15	4.88
P...X	4.19	4.17 (4.30)	4.75 (4.85)	4.24	4.45	4.26	4.29	4.27
(c) Dihedral Angles (deg) ^f								
A–B	29.4	3.2 (6.2)	1.9 (3.3)	25.3	40.5	19.0	14.0	9.8
A'–B	26.9	2.5 (10.1)	1.9 (8.0)	9.6	11.0	13.3	15.9	24.5

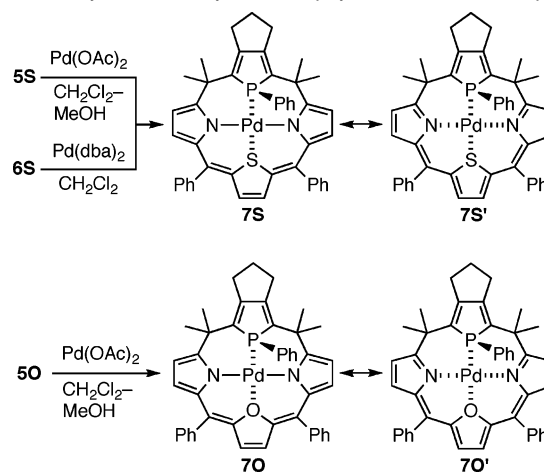
^a Data in parentheses are those of pairing molecules. ^b $ML_n = RhCl(CH_2Cl)$. ^c $ML_n = RhCl_2$. ^d $ML_n = AuCl$. ^e The average values between *y* and *y'* are listed (*y* denotes *d–k*). ^f Dihedral angles between the mean planes A/A' and B.

oriented inside the core, and different types of macrocyclic coordination sites consisting of P, N, O, and S donors are constructed.

The phosphole-containing hybrid calixpyrins **3–6** are air-stable, orange or purple solids, and are soluble in many organic solvents including $CHCl_3$, CH_2Cl_2 , THF, and toluene. As shown in Figure 5a, the UV–vis absorption spectra of **5** and **6** in CH_2Cl_2 display broad absorption bands due to π – π^* transitions at around 400–600 nm. The 16π -conjugated hybrids **6S** and **6N** showed the absorptions at longer wavelengths as compared to those of the 14π -conjugated hybrids **5S** and **5O**. The spectral shape of **6S** is slightly different from that of **6N**, implying that the character of the vibronic states of the N–X–N moiety is affected by the nature of the central heteroles.

III. Complexation of Phosphole-Containing Hybrid Calixpyrins. To obtain fundamental information on the coordinating properties of the phosphole-containing hybrid calixpyrins, we examined the complexation reactions of **5O**, **5S**, **6S**, and **6N** with palladium, rhodium, and gold (Schemes 3–5), and the whole results are summarized in Scheme 6.

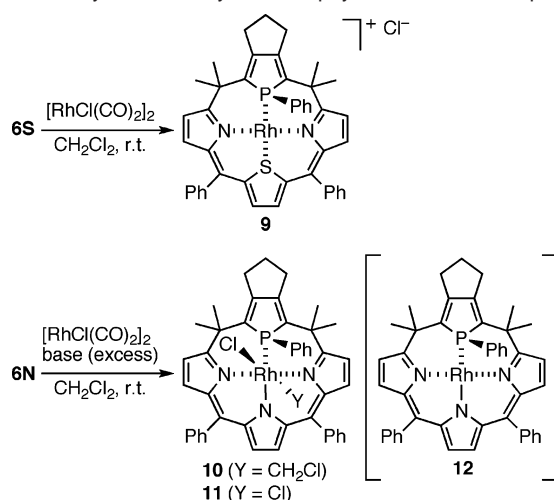
A. Palladium Complexes. Treatment of the 14π - σ^3 -P,-(NH)₂-S-hybrid **5S** with $Pd(OAc)_2$ in CH_2Cl_2 –MeOH at room temperature afforded P,N₂-S-hybrid calixpyrin–palladium complex **7S** as an air-stable, purple solid in 93% yield. Notably, the reaction of the 16π - σ^3 -P,N₂-S-hybrid **6S** with $Pd(dba)_2$ (*dba* = dibenzylideneacetone) produced the same complex, **7S**, in 92% yield (Scheme 3). These results indicate that the hybrid calixpyrins behave as redox-active macrocyclic ligands. That

Scheme 3. Synthesis of Hybrid Calixpyrin–Palladium Complexes

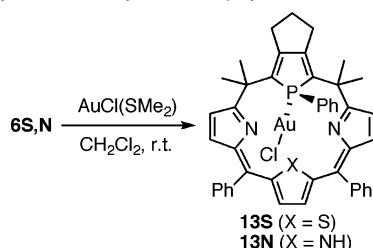
is, the electron transfer between the π -conjugated N–S–N unit and the palladium center occurs in the complexation, when thermodynamically possible (*vide infra*). The σ^3 -P,(NH)₂-O-hybrid **5O** also reacted with $Pd(OAc)_2$ at room temperature to give the P,N₂-O-hybrid calixpyrin–palladium complex **7O** as a purple solid in 72% yield. In the UV–vis absorption spectra in CH_2Cl_2 , both **7O** and **7S** showed broad absorptions at around 500–600 nm (Figure 5b).

In the ¹H NMR spectrum of **7O** in $CDCl_3$, the pyrrole- β and furan- β protons were observed at δ 5.40–6.60 ppm as significantly broadened peaks, implying that the conformational

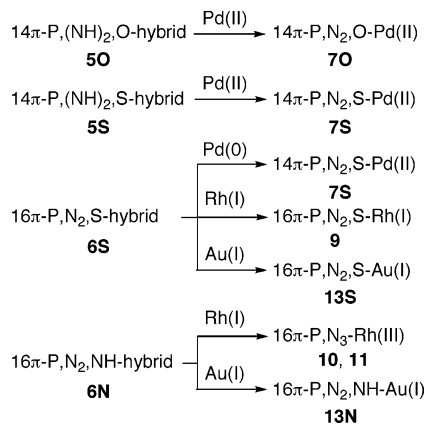
Scheme 4. Synthesis of Hybrid Calixphyrin–Rhodium Complexes



Scheme 5. Synthesis of Hybrid Calixphyrin–Gold Complexes



Scheme 6. Summary of Complexation Reactions of Phosphole-Containing Hybrid Calixphyrins



mobility at the N–O–N unit is restrained. In DMSO-*d*₆, however, **7O** showed relatively sharp peaks due to the respective β protons at δ 5.96 and 5.53 ppm. The ¹H NMR spectrum of **7S** in CDCl₃ showed the pyrrole-β protons at δ 6.10 and 6.22 ppm and the thiophene-β protons at δ 6.34 ppm, which are close to the corresponding chemical shifts of **5S** rather than those of **6S**. The ³¹P NMR peaks of **7O** and **7S** in CDCl₃ were observed at δ 60.5 and 47.0 ppm, respectively. A large difference in the ³¹P chemical shifts may be relevant to the different trans influence from the chalcogen atoms of the central heterole rings in the N–X–N units.

The structures of **7O** and **7S** were elucidated by X-ray crystallographic analyses (Table S1 in Supporting Information and Figures 6 and 7). In each complex, the palladium center is coordinated by the phosphorus, two nitrogen, and sulfur/oxygen atoms at the core to adopt a square planar geometry ($\Sigma_{\text{L-Pd-L}'} = \text{ca. } 360^\circ$). The twisted N–O–N conformation of **7O**

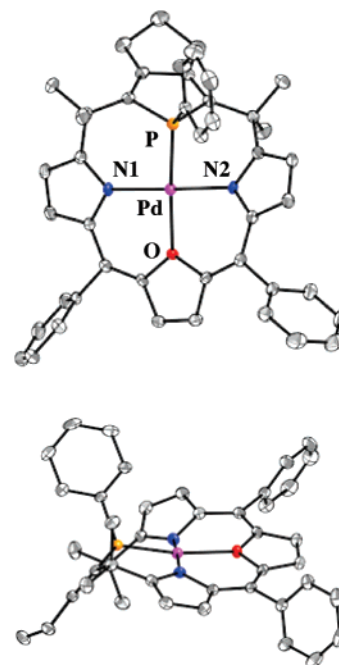


Figure 6. Top and side views of **7O** (50% probability ellipsoids). Hydrogen atoms and a solvent molecule are omitted for clarity: gray (C), blue (N), purple (Pd), red (O), orange (P). Selected bond lengths (Å) and bond angles (deg): Pd–P, 2.1459(7); Pd–N(1), 2.035(2); Pd–N(2), 2.050(2); Pd–O, 2.1098(17); N1–Pd–P, 85.74(6); N1–Pd–O, 89.94(7); N2–Pd–P, 93.70(6); N2–Pd–O, 91.40(7). $\Sigma_{\text{C-P-C}} = 316.8^\circ$.

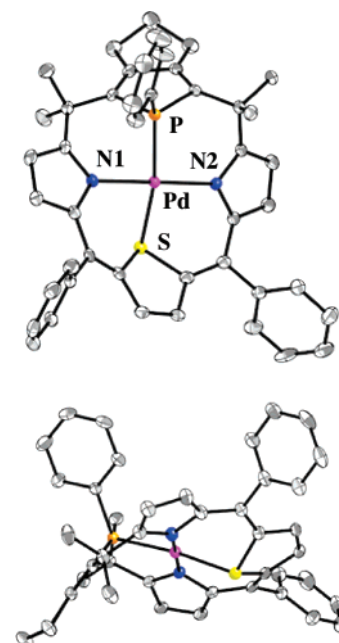
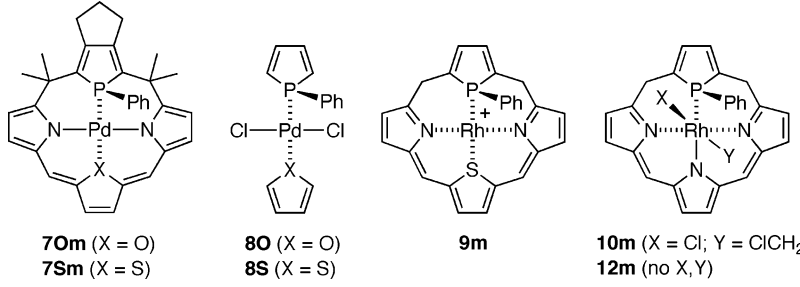


Figure 7. Top and side views of **7S** (50% probability ellipsoids). Hydrogen atoms are omitted for clarity: gray (C), blue (N), orange (P), yellow (S), purple (Pd). Selected bond lengths (Å) and bond angles (deg): Pd–P, 2.2135(8); Pd–N(1), 2.079(2); Pd–N(2), 2.066(3); Pd–S, 2.2667(8); N1–Pd–P, 95.21(7); N1–Pd–S, 92.93(6); N2–Pd–P, 85.75(7); N2–Pd–S, 85.77(7). $\Sigma_{\text{C-P-C}} = 319.4^\circ$.

resembles that observed for the free base **5O**. As listed in Table 1, the dihedral angles between the pyrrole and furan rings as well as the meso–meso distances of **7O** are comparable or somewhat smaller than the respective values of **5O**. The complex **7S** adopts a similar conformation, where the N–S–N unit is not on the same plane. As the pyrrole rings are

Table 2. NAO Occupancies of d Orbitals for Model Complexes^a


	NAO occupancies						
	7Om	8O	7Sm	8S	9m	10m	12m
d_{xy}	1.963	1.975	1.960	1.976	1.928	1.964	1.938
d_{yz}	1.975	1.995	1.976	1.994	1.924	1.949	1.899
d_{zx}	1.944	1.963	1.963	1.967	1.916	1.925	1.783
$d_{x^2-y^2}$	1.183	1.191	1.233	1.235	0.943	1.030	0.905
d_z^2	1.929	1.955	1.935	1.960	1.820	1.241	1.885

^a For directions of x , y , z axes, see Figures S4 and S6 in the Supporting Information.

significantly tilted from the thiophene mean plane with dihedral angles of 11.0–40.5°, the meso–meso distances a – c of **7S** differ considerably from those of the free base **6S**.

In complexes **7O** and **7S**, the phosphole ring leans toward the inside for binding the palladium. As a result, dihedral angles between the phosphole ring and a mean plane formed by the four meso carbon atoms (45.6° for **7O** and 50.9° for **7S**) become more acute in comparison with those of the corresponding free bases (64.0° for **5O** and 85.1° for **6S**). To keep the square planar geometry at the palladium center in the P,N₂,S-hybrid core, the sulfur atom in **7S** is deviated from the thiophene mean plane by 0.13 Å. The N···N distances of **7O** (4.08 Å) and **7S** (4.15 Å) are shorter by 0.51–0.67 Å than those of **5O** (4.59 Å) and **6S** (4.82 Å), because two covalent bonds are formed between the palladium and the two nitrogen atoms in these palladium complexes. It is evident that the calixphyrin platform varies its shape flexibly to provide the most suitable coordination environment for the central metal. The Pd–N bond lengths [2.066(2)–2.079(2) Å] and the Pd–P bond length [2.2135(8) Å] of **7S** are slightly longer than those of **7O** [Pd–N, 2.035(2)–2.050(2) Å; Pd–P, 2.1459(7) Å], reflecting the difference in core sizes of their hybrid ligands. The Pd–N bond lengths of **7O** and **7S** are somewhat longer than the typical values (2.012 ± 0.018 Å) observed for Pd-coordinated porphyrin-type macrocycles.²⁸

As mentioned above, the carbon–carbon/nitrogen bond alternation at the N–X–N units (X = O, S) is a good probe for evaluating the oxidation state at their π -conjugated systems. In the complexes **7O** and **7S**, the difference in bond lengths at d – h is very small ($\Delta L = 0.01$ – 0.03 Å), suggesting high aromaticity at the pyrrole rings. By contrast, the bond lengths at i and k are longer by 0.08–0.1 Å than those at j and l , implying that the double bond character at j and l is much larger than that of the adjacent carbon–carbon bonds. These data are indicative of noticeable contribution by the canonical structures **7O** and **7S**, in which the formal oxidation states of Pd and the P,N₂,X-hybrid ligands are considered to be +2 and –2, respectively. Thus, the contribution by another canonical structures **7O'** and **7S'** seems to be very little, if any.

The electrochemical measurements made this point more concisely and unequivocally. As shown in Figure S3, the electrochemical oxidation processes of **5S** and **7S** were observed as similar reversible waves in their cyclic voltammograms (in CH₂Cl₂ using 0.1 M *n*-Bu₄NPF₆ as an electrolyte). The first and second oxidation potentials ($E_{\text{ox},1}$ and $E_{\text{ox},2}$ vs FeCp*₂/FeCp*₂⁺; Cp* = C₅Me₅) determined by differential pulse voltammetry (DPV) are +0.34 and +0.54 V for **5S** and +0.23 and +0.34 V for **7S**, respectively. Both of the oxidation processes of **7S** occurred at the more positive potentials than those of **5S**, indicating that the N–S–N unit in the Pd complex **7S** is oxidized more easily than that in the free base **5S**. In contrast to **5S** and **7S**, the σ^3 -P,N₂,S-hybrid **6S** did not show any oxidation processes in the same region (–0.37 to ca. +0.6 V vs Ag/Ag⁺; 0.0 to ca. +0.97 V vs FeCp*₂/FeCp*₂⁺). Therefore, we can safely conclude that the N–S–N unit in **7S** possesses a 14 π character like that in **5S**.

To get more insight into the formal oxidation state of the palladium center in **7O** and **7S**, we carried out DFT calculations on complexes **7Xm** and **8X** (X = O, S), which were adopted as models for **7X** and Pd(II) references, respectively (Table 2 and Figure S4). Except for hydrogen, the geometries of **7Xm** were taken to be the same as the experimentally characterized geometries of **7X**, while the positions of the hydrogen atoms of **7Xm** were optimized by the molecular mechanics with a universal force field (UFF).²⁹ The geometries of **8X** were optimized with the DFT method.

As shown in Table 2, the natural atomic orbital (NAO) occupancies³⁰ of the $d_{x^2-y^2}$ orbitals were calculated to be 1.183e for **7Om** and 1.233e for **7Sm**, which are almost the same as the corresponding values of the Pd(II) reference compounds **8O** (1.191e) and **8S** (1.235e) (see Figure S4 for coordinate system of these complexes).³¹ Also, the LUMO of **7Xm** consists of the $d_{x^2-y^2}$ orbital similar to that of **8X**, where the π^* orbital of the phosphole moiety somewhat mixes into the LUMO probably because the π^* orbital is in the same symmetry as the $d_{x^2-y^2}$

(29) Rappé, A. K.; Casewit, C. J.; Colwell, K. S.; Goddard, W. A., III; Skiff, W. M. *J. Am. Chem. Soc.* **1992**, *114*, 10024–10035.

(30) Reed, A. E.; Curtis, L. A.; Weinhold, F. *Chem. Rev.* **1988**, *88*, 899–926 and references therein.

(31) As we recalculated the NAO occupancies for **7Sm** and **8S** using a different basis set, the values listed in Table 2 are slightly different from those reported in ref 20.

(28) Liu, D.; Ferrence, G. M.; Lash, T. D. *J. Org. Chem.* **2004**, *69*, 6079–6093 and references therein.

orbital and at a higher energy than the LUMO (Figure S4). The other four d orbitals are involved in the occupied molecular orbitals of both **7Xm** and **8X**. These results strongly support the fact that the palladium center in **7X** takes a +2 oxidation state in a formal sense and that the N–X–N units possess the 14 π -conjugated structure, as were suggested by X-ray crystallography and electrochemical measurements. Thus, the P,N₂,O- and P,N₂,S-hybrid calixphyrin platforms behave as tetradentate, dianionic ligands in the respective palladium complexes **7O** and **7S**. It must be emphasized again that the Pd(II) complex **7S** is formed exclusively by the reaction between **6S** and Pd(dba)₂. This result indicates that the palladium is oxidized from 0 to +2 by the 16 π -conjugated N–S–N unit of **6S** in the complexation. Such reactivity can be reasonably explained by considering the ideal number of d electrons at the metal center in stable, square planar palladium complexes.

B. Rhodium Complexes. Next, we examined the complexation of **6S** and **6N** with a rhodium(I) salt (Scheme 4). Treatment of the σ^3 -P,N₂,S-hybrid **6S** with a half equiv of [RhCl(CO)₂]₂ (1 equiv for Rh) in CH₂Cl₂ at room temperature afforded the Rh–P,N₂,S-hybrid complex **9** as a purple solid in 87% yield. The Rh complex **9** is sparingly soluble in diethyl ether and shows a much lower *R_f* value (~0) on silica-gel TLC as compared to that (*R_f* ≈ 0.5) observed for the Pd complex **7S** under the same conditions (eluted with hexane/EtOAc, 4/1). The MS spectrum of **9** displayed a strong ion peak at *m/z* 774, which corresponds to the [M – Cl]⁺ ion. Presumably, the chlorine atom in **9** is loosely bound to the rhodium if at all. Thus, it could be an ionic complex. In the ³¹P NMR spectrum of **9**, a characteristic doublet peak was observed at δ 69.6 ppm with a ³¹P–¹⁰³Rh coupling constant of 171 Hz, implying that the formal oxidation state of the rhodium center is +1.³² This was supported by the theoretical calculations on a cationic model complex **9m**, in which the NAO occupancy of the *d_{x²-y²}* orbital is much smaller than those of the other four d orbitals (Table 2 and Figure S6a). Unlike the complexation with Pd(dba)₂, the reduction of the 16 π -N–S–N unit does not occur, and the calixphyrin platform in **9** seems to behave as a neutral, tetradentate P,N₂,S-ligand.

In sharp contrast to **6S**, the σ^3 -P,N₂,NH-hybrid **6N** showed an unexpected reactivity. Upon adding a CH₂Cl₂ solution of Et₃N to a mixture of **6N** and [RhCl(CO)₂]₂, the color of the solution changed instantaneously from red to blue, affording the rhodium(III) complex **10** as a deep blue solid in 79% yield. When K₂CO₃ was used in place of Et₃N, **10** was formed in 32% yield together with a similar amount of the rhodium(III) complex **11**. In the ³¹P NMR spectra of **10** and **11**, a diagnostic doublet peak was observed at δ 67.3 ppm (¹*J*_{P–Rh} = 98 Hz) and 62.6 ppm (¹*J*_{P–Rh} = 92 Hz), respectively, supporting the rhodium +3 oxidation state. In the ¹H NMR spectrum of **10**, the rhodium-bound methylene protons were observed as a pseudotriplet at δ 3.48 ppm (²*J*_{H–Rh} = ³*J*_{H–P} = 3.0 Hz). As shown in Figure 5b, the Rh(III) complexes **10** and **11** showed broad absorptions at 600–750 nm in CH₂Cl₂. The absorption maxima observed for **10** (692 nm) and **11** (684 nm) are red-shifted by 145–153 nm as compared to that observed for the Rh(I) complex **9** (539 nm), indicating that the oxidation state of the rhodium center considerably affects the π – π^* transitions of the N–X–N units in the calixphyrin platforms.

(32) Brown, T. H.; Green, P. J. *J. Am. Chem. Soc.* **1970**, *92*, 2359–2362.

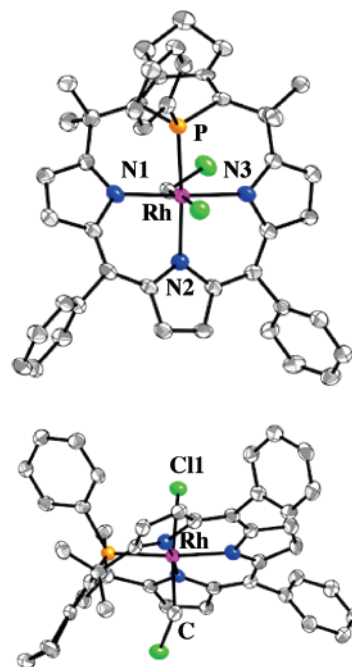


Figure 8. Top and side views of **10** (50% probability ellipsoids). Hydrogen atoms and a solvent molecule are omitted for clarity: gray (C), blue (N), orange (P), green (Cl), purple (Rh). Selected bond lengths (Å) and bond angles (deg): Rh–P, 2.2042(12); Rh–N1, 2.079(3); Rh–N2, 2.062(4); Rh–N3, 2.081(4); Rh–Cl1, 2.4584(12); Rh–C, 2.073(4); N1–Rh–P, 93.48(10); N1–Rh–N2, 91.78(15); N3–Rh–P, 84.39(11); N3–Rh–N2, 90.77(15); Cl1–Rh–C, 173.44(13). $\Sigma_{C-P-C} = 313.2^\circ$.

The structures of **10** and **11** were successfully elucidated by X-ray crystallography. As shown in Figures 8 and S5, the rhodium center in each complex adopts a distorted octahedral geometry with the macrocyclic P,N₃-platform at the equatorial sites, wherein the N–N–N units are not on the same plane to avoid steric congestion at the core. The two 2-azafluvene rings are twisted from the central pyrrole ring with dihedral angles of 13.3–19.0° for **10** and 14.0–15.9° for **11**. The Rh–N bond lengths [2.062(4)–2.082(4) Å for **10** and 2.068(4)–2.082(4) Å for **11**] are at the long end of the range of typical values (2.00–2.08 Å) reported for Rh(III)-coordinated porphyrin-type macrocycles.³³ The axial chloromethyl group in **10** is located at the opposite side to the P-phenyl group with a Rh–C bond length of 2.073(4) Å and a C–Rh–Cl bond angle of 173.44(13)°. The Rh–Cl bond length of **10** [2.4584(12) Å] is appreciably longer than those of **11** [2.3527(13) and 2.3490(13) Å], reflecting the difference in trans influence between the chloromethyl group in **10** and the chlorine atom in **11**. The bond alternation at the N–N–N units of **10** and **11**, which is similar to that of **6N**, represents a significant contribution of the 16 π -conjugated structure. Therefore, the P,N₃-hybrid calixphyrin platform in these complexes is regarded as a monoanionic, tetradentate P,N₃-ligand.

The above results demonstrate that the reactivity at the rhodium center coordinated by the phosphole-containing hybrid calixphyrins can be varied largely by changing the central heterole (X) of the π -conjugated N–X–N unit. It is most likely

(33) For example, see: (a) Fleischer, E. B.; Lavalley, D. *J. Am. Chem. Soc.* **1967**, *89*, 7132–7133. (b) Hanson, L. K.; Gouterman, M.; Hanson, J. C. *J. Am. Chem. Soc.* **1973**, *95*, 4822–4829. (c) Takenaka, A.; Syal, S. K.; Sasada, Y.; Omura, T.; Ogoshi, H.; Yoshida, Z.-I. *Acta Crystallogr.* **1976**, *B32*, 62–65. (d) Latos-Grażyński, L.; Lisowski, J.; Olmstead, M. M.; Balch, A. L. *Inorg. Chem.* **1989**, *28*, 3328–3331.

that a neutral Rh(I) complex **12** is initially generated from the P,N₂,NH-hybrid **6N**, [RhCl(CO)₂]₂, and a base. Thus, the Rh(III) complex **10** would be formed via oxidative addition of the C–Cl bond of dichloromethane onto the Rh(I) center in **12**. However, all attempts to isolate **12** using other solvents have been unsuccessful, probably because of its extremely high reactivity. To evaluate a driving force for this step, DFT calculations were performed on model complexes **10m** and **12m** (for details, see Supporting Information). As shown in Scheme S1, **10m** is formed from **12m** and CH₂Cl₂ with a large stabilization energy of 18.5 kcal mol⁻¹, suggesting that the C–Cl bond activation of dichloromethane by **12** is a thermodynamically favorable process. The NAO occupancies of d orbitals of the model complexes **10m** and **12m** represent that the formal oxidation states of their rhodium centers are +3 and +1, respectively (Table 2 and Figure S6b,c).

It is well-known that the C–Cl bond of chloroalkanes is activated at the nucleophilic Rh(I) center supported by electron-rich N, P, and/or S donors.³⁴ The previously reported C–Cl bond activation of dichloromethane by Rh(I) complexes bearing neutral P,N₂- and N₃-ligands takes about 16–24 h to complete the reaction.^{34c–e} In marked contrast, the formation of **10** from **6N** was complete *within a few seconds* at room temperature.³⁵ In this context, the P,N₃-hybrid calixphyrin monoanion provides a remarkably high nucleophilicity at the rhodium(I) center coordinated in the core.

C. Gold Complexes. In the complexation with AuCl(SMe₂), both **6S** and **6N** behaved as monophosphine ligands to yield the corresponding Au(I)–phosphole complexes **13S** and **13N** in 83 and 85% yield, respectively (Scheme 5). The ³¹P NMR spectra of **13S** and **13N** in CDCl₃ showed singlet peaks at δ 58.0 and 58.1 ppm, respectively. In their ¹H NMR spectra, the β protons derived from the N–X–N units (δ 6.55–6.70 ppm for **13S**; δ 5.97–6.69 ppm for **13N**) and the pyrrole NH proton of **13N** (δ 11.41 ppm) were observed at almost the same regions as those of the corresponding free bases **6S** and **6N**, supporting the fact that the N–X–N units are not involved in the coordination sphere at the gold center.

The structure of **13S** was further determined by X-ray crystallography. As depicted in Figure 9, the gold center is coordinated by the phosphorus atom with a P–Au bond length of 2.2319(9) Å and a P–Au–Cl bond angle of 177.52(3)°, which are close to the corresponding values reported for Au(I)–phosphole (monophosphine) complexes.³⁶ Owing to this coordination, the phosphole ring is perpendicular to a mean plane formed by the four meso carbons. The carbon–carbon/nitrogen bond alternation at the 16π-N–S–N unit as well as the meso–meso and N···N distances of **13S** is very close to

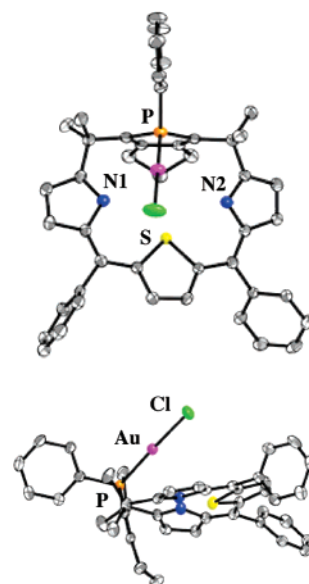


Figure 9. Top and side views of **13S** (50% probability ellipsoids). Hydrogen atoms are omitted for clarity: gray (C), blue (N), orange (P), yellow (S), green (Cl), purple (Au). Selected bond lengths (Å) and bond angles (deg): Au–P, 2.2319(9); Au–Cl, 2.2932(9); P–Au–Cl, 177.52(3). $\Sigma_{C-P-C} = 307.1^\circ$.

that observed for **6S** (Table 1), which well explains the ¹H NMR observations.

IV. Catalytic Activities of Phosphole-Containing Hybrid Calixphyrin–Metal Complexes. To shed light on the catalytic activities of the phosphole-containing hybrid calixphyrin–metal complexes, we examined typical Pd- and Rh-catalyzed organic transformations using **7O**, **7S**, and **6X**/[RhCl(CO)₂]₂ (X = S, N) as catalysts. At the resting state, the metal center is tightly coordinated by the four heteroatoms at the core in the calixphyrin platform. If the metal center is dissociated partially from the macrocyclic donors by a flipping motion, however, a coordinatively unsaturated, reactive metal center may be generated. It was therefore anticipated that the phosphole-containing hybrid calixphyrins would behave as hemilabile P,N₂,X-mixed donor ligands for transition metals under appropriate reaction conditions. More importantly, it was expected that changing the combination of the N–X–N unit would give rise to diverse reactivities at the metal center, because the charge and the σ-donating and π-accepting abilities of the heteroatom donors vary significantly as mentioned in the Introduction.

A. Palladium Catalysts for Coupling Reactions. The hemilability of the hybrid calixphyrin platforms was examined by variable-temperature (VT) NMR measurements on the Pd–P,N₂,X-hybrid complexes **7O** and **7S**. When heated at 125 °C in DMSO-*d*₆, the pyrrole-β and furan-β protons of **7O** were slightly shifted and broadened as compared to those observed at 25 °C (Figure S7a). When cooled down to room temperature, the relatively sharp peaks due to the resting state of **7O** reappeared. A similar temperature-dependence of the NMR

(34) For example, see: (a) Collman, J. P.; Murphy, D. W.; Dolcetti, G. *J. Am. Chem. Soc.* **1973**, *95*, 2687–2689. (b) Marder, T. B.; Fultz, W. C.; Calabrese, J. C.; Harlow, R. L.; Milstein, D. *J. Chem. Soc., Chem. Commun.* **1987**, 1543–1545. (c) Nishiyama, H.; Horiata, M.; Hirai, T.; Wakamatsu, S.; Itoh, K. *Organometallics* **1991**, *10*, 2706–2708. (d) Haarman, H. F.; Ernsting, J. M.; Kranenburg, M.; Kooijman, H.; Veldman, N.; Spek, A. L.; van Leeuwen, P. W. N. M.; Vrieze, K. *Organometallics* **1997**, *16*, 887–900. (e) Koshevoy, I. O.; Tunik, S. P.; Poë, A. J.; Lough, A.; Pursiainen, J.; Piriilä, P. *Organometallics* **2004**, *23*, 2641–2650. (f) Germoni, A.; Deschamps, B.; Ricard, L.; Mercier, F.; Mathey, F. *J. Organomet. Chem.* **2005**, *690*, 1133–1139. (g) Sharp, P. R. In *Comprehensive Organometallic Chemistry II*; Abel, E. W., Stone, F. G. A., Wilkinson, G., Eds.; Pergamon: Oxford, England, 1995; Vol. 8, pp 115–302 and references therein.

(35) When the complexation between **6N** and [RhCl(CO)₂]₂ was carried out in toluene, the Rh(III) complex **11** was obtained in ca. 30% yield.

(36) (a) Attar, S.; Bearden, W. H.; Alcock, N. W.; Alyea, E. C.; Nelson, J. H. *Inorg. Chem.* **1990**, *29*, 425–433. Au–P, 2.220(9)–2.227(2) Å; P–Au–Cl, 172.4(1)–178.8(1)°. (b) Su, H.-C.; Fadhel, O.; Yang, C.-J.; Cho, T.-Y.; Fave, C.; Hissler, M.; Wu, C.-C.; Réau, R. *J. Am. Chem. Soc.* **2006**, *128*, 983–995. Au–P, 2.2290(16)–2.2300(16) Å; P–Au–Cl, 171.64(7)–174.63(8)°. (c) Dienes, Y.; Eggenstein, M.; Neumann, T.; Englert, U.; Baumgartner, T. *Dalton Trans.* **2006**, 1424–1433. Au–P, 2.2249(12) Å; P–Au–Cl, 177.26(4)°.

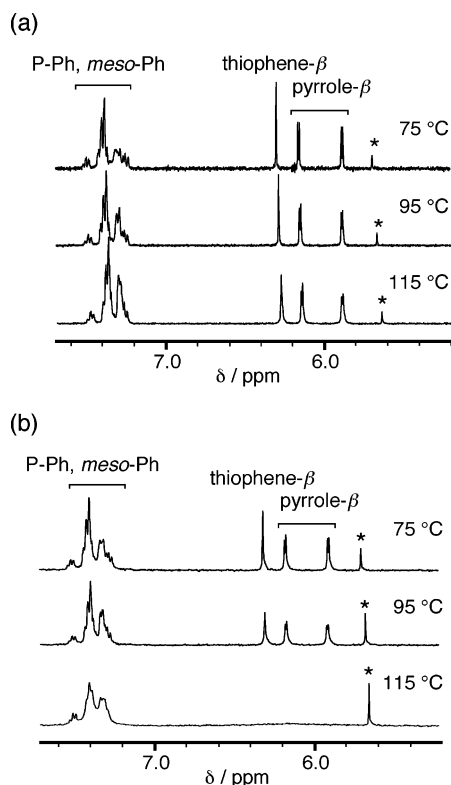


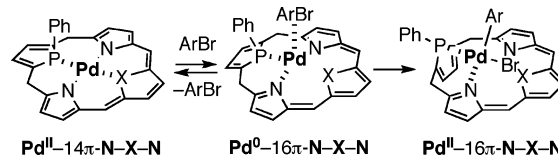
Figure 10. Variable-temperature ^1H NMR spectra of **7S** in $\text{DMSO-}d_6$: (a) in the absence of *p*-iodonitrobenzene; (b) in the presence of *p*-iodonitrobenzene. Asterisks (*) indicate a residual peak of CH_2Cl_2 .

spectra was observed for **7S** in $\text{DMA-}d_9$ (Figure S7b). The coordination environment in **7X** ($\text{X} = \text{O}, \text{S}$) becomes dynamic at high temperatures, which may allow for partial dissociation of the heteroatom donors and for coordinative interaction of the face-up palladium center with the solvents.³⁷

In the VT NMR spectra of a $\text{DMSO-}d_6$ solution containing **7S** and excess *p*-iodonitrobenzene at 115°C , we could not assign the heterole- β protons because of their significant broadening (Figure 10b). This is in sharp contrast to the result observed for the iodide-free solution of **7S** at the same temperature, which displays distinct peaks due to the β protons at δ 5.8–6.3 ppm (Figure 10a). When the iodide-containing solution was cooled down to room temperature, the peaks due to **7S** appeared reversibly. These findings suggested to us that the iodoarene interacts with the palladium center in **7S** at elevated temperatures.

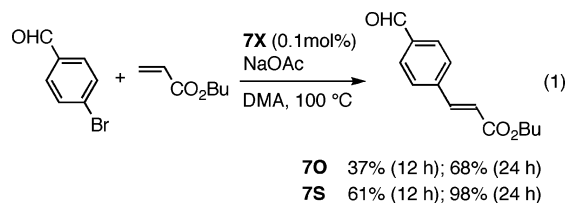
Although there is no direct experimental evidence regarding aryl–palladium(II)–halide species at present,³⁸ we expected that the $\text{Pd-P,N}_2\text{X}$ -hybrid complexes could activate the carbon–halogen bond by a redox-coupled oxidative addition mechanism, as is illustrated in Scheme 7.³⁹ Thus, under appropriate reaction conditions, dissociation of the furan/thiophene and pyrrole rings

Scheme 7. A Proposed Redox-Coupled Oxidative Addition Mechanism for the $\text{P,N}_2\text{X}$ -Hybrid Calixphyrin–Palladium Complexes



takes place to generate vacant coordination sites at the metal center, accompanied by the reduction of the palladium from +2 to its zero valent state and the oxidation of the N-X-N unit from 14π to 16π . Namely, two electrons that are necessary to oxidatively cleave the carbon–halogen bond are provided by the N-X-N unit through the coordinated palladium center. Such a bond-activating methodology is of interest from a mechanistic point of view, as it highlights the characteristic properties of the hybrid calixphyrin platforms as hemilabile and redox-active ligands.

To verify the above hypothesis, we examined the Heck reaction (Mizoroki–Heck reaction) of *p*-bromobenzaldehyde with *n*-butyl acrylate in *N,N*-dimethylacetamide at 100°C using the palladium complexes **7O** and **7S** as catalysts (eq 1).⁴⁰ As expected, the coupling reaction proceeded at 100°C in the presence of 0.1 mol% of **7O** or **7S** to afford the Heck product in 68–98% yields (turnover numbers = 680–980 after 24 h)⁴¹ without the deposition of observable quantities of palladium black. The $\text{Pd-P,N}_2\text{S}$ -hybrid complex **7S** catalyzed the reaction more rapidly than the $\text{Pd-P,N}_2\text{S}$ -hybrid complex **7O**, although the differences in the observed rate constants are small. The present Heck reaction seems to operate through a commonly admitted Pd(0)-Pd(II) catalytic cycle,⁴² which might involve the proposed redox-coupled oxidative addition step.



B. Rhodium Catalysts for Hydrosilylation. We next examined the Rh-catalyzed hydrosilylations of a ketone and an acetylene using the $\text{Rh-P,N}_2\text{X}$ -hybrid calixphyrin complexes generated from $\mathbf{6X}/[\text{RhCl}(\text{CO})_2]_2$ ($\text{X} = \text{S}, \text{N}$). Treatment of acetophenone with Ph_2SiH_2 in the presence of 0.5/0.25 mol % of $\mathbf{6N}/[\text{RhCl}(\text{CO})_2]_2$ in THF for 6 h at room temperature afforded 1-phenylethanol in 91% yield after hydrolysis (eq 2). When **6S** was used in place of **6N**, the rate of hydrosilylation

(37) Slow exchange may occur between two coordination states, in which the pyrrole ligands are bound to the palladium non-equivalently.

(38) We are planning to perform theoretical study on the oxidative addition of a phenyl halide to $\text{P,N}_2\text{X}$ -hybrid complexes in detail, to clarify the nature of the active species.

(39) Recently, Heyduk and co-workers reported the redox-based bond-making and bond-breaking reactions using a zirconium(IV) redox-active ligand (2,4-di-*tert*-butyl-6-*tert*-butylamidophenolate) complex. See: (a) Blackmore, K. J.; Ziller, J. W.; Heyduk, A. F. *Inorg. Chem.* **2005**, *44*, 5559–5561. (b) Haneline, M. R.; Heyduk, A. F. *J. Am. Chem. Soc.* **2006**, *128*, 8410–8411.

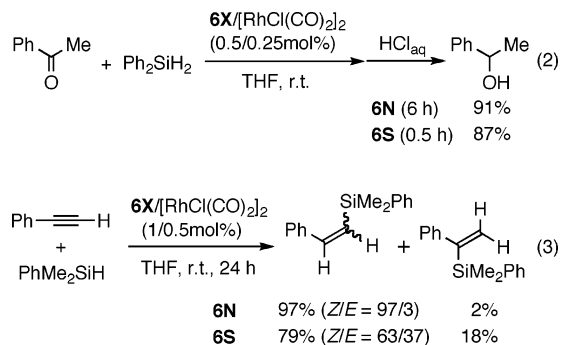
(40) Recent reviews on the nature of the active species in palladium-catalyzed coupling reactions have pointed out that nearly all Pd precatalysts decompose at high temperatures (e.g., $> 120^\circ\text{C}$) to liberate soluble “ligand-free” palladium colloids or nanoparticles. To avoid this uncertainty, the present Heck reactions were conducted at 100°C . (a) Beletskaya, I. P.; Cheprakov, A. V. *J. Organomet. Chem.* **2004**, *689*, 4055–4082. (b) de Vries, J. G. *Dalton Trans.* **2006**, 421–429. (c) Phan, N. T. S.; van der Sluys, M.; Jones, C. W. *Adv. Synth. Catal.* **2006**, *348*, 609–679. (d) Weck, M.; Jones, C. W. *Inorg. Chem.* **2007**, *46*, 1865–1875.

(41) In our preliminary communication (ref 20), we reported the results on the same Heck reaction conducted at 135°C , which gave the turnover number of 9700 after 4 h.

(42) For example, see: (a) Heck, R. F. *Acc. Chem. Res.* **1979**, *12*, 146–151. (b) Crisp, G. T. *Chem. Soc. Rev.* **1998**, *27*, 427–436. (c) Beletskaya, I. P.; Cheprakov, A. V. *Chem. Rev.* **2000**, *100*, 3009–3066. (d) Amatore, C.; Jutand, A. *Acc. Chem. Res.* **2000**, *33*, 314–321.

was accelerated dramatically (87% yield after 0.5 h).⁴³ Although we cannot define the exact nature of the intermediate, the electronic character at the rhodium center in the $6\mathbf{X}/[\text{RhCl}(\text{CO})_2]_2$ systems may be reflected in their catalytic activities.⁴⁴ Note that the catalytic activity observed for $\mathbf{9}$, generated from $6\mathbf{S}$ and $[\text{RhCl}(\text{CO})_2]_2$, is as efficient as those reported for highly active rhodium catalysts bearing neutral, multidentate N_3 -^{44b,c} or P,X-mixed donor ligands (X =, N, S).⁴⁵

The high catalytic activity of $6\mathbf{X}/[\text{RhCl}(\text{CO})_2]_2$ (X = S, N) was also attained in the hydrosilylation of phenylacetylene with PhMe_2SiH , which resulted in the formation of a mixture of styrylsilanes (eq 3). It has been proposed that the *Z/E* stereoselectivity of β -silylstyrenes is a good index to evaluate the electronic character at the rhodium(I) center. Namely, the hydrosilylation of terminal alkynes catalyzed by neutral rhodium complexes displays high *Z* selectivity, whereas that catalyzed by cationic rhodium complexes exhibits high *E* selectivity.^{46,47} As listed in eq 3, a high *Z/E* selectivity (97/3) as well as a high β/α selectivity (98/2) was achieved in the reaction with $6\mathbf{N}$, implying that the Rh–P,N₃-hybrid catalyst operates as a totally neutral Rh complex. On the other hand, a low *Z/E* selectivity (63/37) was observed for the reaction using $6\mathbf{S}$, suggesting that the rhodium center in the Rh–P,N₂,S-hybrid catalyst possesses a cationic character in some extent (vide supra). In both catalyst systems, the *Z/E* ratios were constant during the reaction.



Conclusions

We have systematically investigated the syntheses, structures, and coordinating properties of 5,10-porphodimethene-type phosphole-containing hybrid calixphyrins for the first time. It has

been elucidated that the core size, π -conjugated structure, and conformation of the calixphyrin platform vary widely depending on the exquisite combination of heterole subunits in the redox active π -conjugated N–X–N framework. It is of interest that the 14π -P,(NH)₂,X- and 16π -P,N₂,X-hybrid ligands exhibit different coordinating properties in the complexation with palladium, rhodium, and gold. It is also important to note that the hybrid calixphyrin–palladium and –rhodium complexes catalyze the Heck reaction and hydrosilylations, respectively, with high efficiency. To our knowledge, these are the first catalytic processes occurring at the palladium or rhodium center coordinated by macrocyclic, tetradentate P,N₂,X-mixed donor ligands. The present results demonstrate the potential utility of the phosphole-containing hybrid calixphyrins as highly promising hemilabile macrocyclic ligands for the construction of efficient transition-metal catalysts. As the number of combination of heterocycles is unlimited, there is ample room for the synthesis and coordination chemistry of core-modified, hybrid calixphyrins.

Experimental Section

Density Functional Theory (DFT) Calculations on Model Complexes. In the DFT calculations, the B3LYP functional⁴⁸ was used for the exchange-correlation term and two kinds of basis set systems were employed. The smaller system (BS1) was used for geometry optimization. In BS1, core electrons of Pd (up to 3d) and Rh (up to 3d) were replaced with effective core potentials (ECPs),⁴⁹ and its valence electrons were represented with (311111/22111/411) and (311111/22111/411) basis sets,⁴⁹ respectively. For H, C, N, O, P, S, and Cl, 6-31G(d)⁵⁰ basis sets were employed where the diffuse functions were added to N and Cl atoms. The better basis set system (BS2) was used for evaluation of the energy change and natural atomic orbital (NAO) occupancies.³⁰ In BS2, (311111/22111/411/11) and (311111/22111/411/11) basis sets^{49,51} were employed for Pd and Rh, respectively, where the same ECPs as those of BS1 were employed for core electrons. For H, C, N, O, P, S, and Cl, 6-311G(d)⁵² basis sets were employed where the diffuse functions were added to N and Cl atoms. Zero-point energy was evaluated with the DFT/BS1 method, under the assumption of a harmonic oscillator. The Gaussian 03 program package⁵³ was used in all these calculations and the MOLEKEL program⁵⁴ was employed to draw pictures of molecular orbital.

X-ray Crystallographic Analysis. All measurements were made on a Rigaku Saturn CCD area detector with graphite monochromated Mo K α radiation or a Rigaku RAXIS RAPID imaging plate area detector with graphite monochromated Cu K α radiation. The selected crystallographic data are summarized in Table S1. The structures were solved by direct methods (SIR 92⁵⁵ for $\mathbf{5O}$, $\mathbf{6S}$, and $\mathbf{7O}$; SIR 97⁵⁶ for

- (43) In these reactions, a silyl enol ether was formed as a byproduct, which was converted to the starting substrate, acetophenone, after hydrolysis.
- (44) It was reported that cationic rhodium complexes catalyze the asymmetric hydrosilylation of ketones more efficiently than the less cationic counterparts in terms of both reactivity and selectivity. (a) Hayashi, T.; Yamamoto, K.; Kasuga, K.; Omizu, H.; Kumada, M. *J. Organomet. Chem.* **1976**, *113*, 127–137. (b) Nishiyama, H.; Kondo, M.; Nakamura, T.; Itoh, K. *Organometallics* **1991**, *10*, 500–508. (c) Nishiyama, H.; Yamaguchi, S.; Kondo, M.; Itoh, K. *J. Org. Chem.* **1992**, *57*, 4306–4309.
- (45) (a) Nishibayashi, Y.; Segawa, K.; Ohe, K.; Uemura, S. *Organometallics* **1995**, *14*, 5486–5487. (b) Tao, B.; Fu, G. C. *Angew. Chem., Int. Ed.* **2002**, *41*, 3892–3894. (c) Evans, D. A.; Michael, F. E.; Tedrow, J. S.; Campos, K. R. *J. Am. Chem. Soc.* **2003**, *125*, 3534–3543. (d) Riant, O.; Mostefai, N.; Courmarcel, J. *Synthesis* **2004**, 2943–2958 and references therein.
- (46) Ojima and co-workers interpreted the *Z/E* selectivity by considering zwitterionic rhodium–carbenoid intermediates. For example, see: (a) Ojima, I.; Kumagai, M.; Nagai, Y. *J. Organomet. Chem.* **1974**, *66*, C14–C16. (b) Ojima, I.; Clos, N.; Donovan, R. J.; Ingallina, P. *Organometallics* **1990**, *9*, 3127–3133.
- (47) (a) Doyle, M. P.; High, K. G.; Nesloney, C. L.; Clayton, T. W., Jr.; Lin, J. *Organometallics* **1991**, *10*, 1225–1226. (b) Takeuchi, R.; Nitta, S.; Watanabe, D. *J. Org. Chem.* **1995**, *60*, 3045–3051. (c) Mori, A.; Takahisa, E.; Kajiro, H.; Hirabayashi, K.; Nishihara, Y.; Hiyama, T. *Chem. Lett.* **1998**, 443–444. (d) Faller, J. W.; D'Alliessi, D. G. *Organometallics* **2002**, *21*, 1743–1746. (e) Zeng, J. Y.; Hsieh, M.-H.; Lee, H. M. *J. Organomet. Chem.* **2005**, *690*, 5662–5671.

- (48) (a) Becke, A. D. *Phys. Rev. A* **1988**, *38*, 3098–3100. (b) Becke, A. D. *J. Chem. Phys.* **1993**, *98*, 5648–5652. (c) Lee, C.; Yang, W.; Parr, R. G. *Phys. Rev. B* **1988**, *37*, 785–789.
- (49) Andrae, D.; Haeussermann, U.; Dolg, M.; Stoll, H.; Preuss, H. *Theor. Chim. Acta* **1990**, *77*, 123–141.
- (50) (a) Hehre, W. J.; Ditchfield, R.; Pople, J. A. *J. Chem. Phys.* **1972**, *56*, 2257–2261. (b) Francl, M. M.; Pietro, W. J.; Hehre, W. J.; Binkley, J. S.; Gordon, M. S.; DeFrees, D. J.; Pople, J. A. *J. Chem. Phys.* **1982**, *77*, 3654–3665.
- (51) Martin, J. M. L.; Sundermann, A. *J. Chem. Phys.* **2001**, *114*, 3408–3420.
- (52) Krishnan, R.; Binkley, J. S.; Seeger, R.; Pople, J. A. *J. Chem. Phys.* **1980**, *72*, 650–654.
- (53) Pople, J. A.; et al. *Gaussian 03*; Gaussian, Inc.: Pittsburgh, PA, 2003.
- (54) Flükiger, P.; Lüthi, H. P.; Portann, S.; Weber, J. *MOLEKEL, v4.3 for Scientific Computing*; Manno, Switzerland, 2000–2002. Portman, S.; Lüthi, H. P. *CHIMIA* **2000**, *54*, 766–770.
- (55) SIR92: Altomare, A.; Casciaro, G.; Giacovazzo, C.; Guagliardi, A.; Burla, M.; Polidori, G.; Camalli, M. *J. Appl. Cryst.* **1994**, *27*, 435.
- (56) SIR97: Altomare, A.; Burla, M.; Camalli, M.; Casciaro, G.; Giacovazzo, C.; Guagliardi, A.; Moliterni, A.; Polidori, G.; Spagna, R. *J. Appl. Cryst.* **1999**, *32*, 115–119.

13S; SHELXS-97⁵⁷ for **6N** and **11**) and heavy-atom Patterson methods⁵⁸ (for **10**), respectively, and expanded using Fourier techniques.⁵⁹ In the refinement of **6N**, some non-hydrogen atoms were refined anisotropically, while the rest were refined isotropically. In the refinement of other compounds, non-hydrogen atoms were refined anisotropically. Hydrogen atoms were refined using the rigid model. All calculations were performed using CrystalStructure⁶⁰ crystallographic software package except for refinement, which was performed using SHELXL-97.⁵⁷ Considerably large *R* values and low precisions of the bond lengths relevant to light atoms of **6N** might be due to a poor quality of the crystal used. Reflections of poor internal consistency were rejected at the last stage of refinement, so that the completeness of the measured reflections was reduced to 0.976. The crystals of **6S** and **6N** consist of a pair of two independent molecules, one of which is depicted for each compound in Figures 3 and 4. The distances, bond lengths, and dihedral angles are listed in Table 1. The CIF files of **6S** and **7S** were uploaded as the Supporting Information files in our preliminary communication (ref 20).

VT NMR Measurements: Compound **7X** (3 μ mol) was dissolved in DMSO-*d*₆ or DMA-*d*₉ (ca. 0.6 mL), and the solution was transferred into a sealable NMR tube that was well dried. In the case of the measurement of the iodide-containing solution, a mixture of **7S** (3 μ mol) and *p*-iodonitrobenzene (9 μ mol) was dissolved in DMSO-*d*₆ (ca. 0.6 mL). After four freeze-pump-thaw cycles using a vacuum line, the tube was evacuated and sealed. The samples were measured by ¹H NMR (400 MHz) spectrometer equipped with a temperature-control unit.

Heck Reaction of Bromoarenes. Typical Procedure. *p*-Bromobenzaldehyde (460 mg, 2.5 mmol), anhydrous sodium acetate (250 mg), and the Pd complex **7X** (2.5 μ mol) were placed in a Schlenk flask equipped with a reflux condenser. After repeated degassing, triethylenglycol dimethyl ether (50 μ L, internal standard for GC) and *N,N*-dimethylacetamide (2.5 mL) were injected. *n*-Butyl acrylate (0.43

mL, 3 mmol) was added to the flask at 100 °C, and the resulting mixture was stirred at the same temperature. The consumption of *p*-bromobenzaldehyde was monitored by GC, and the yield of the Heck product was determined by comparison with the internal standard.

Hydrosilylation of Acetophenone Using 6N/[RhCl(CO)₂]₂. The hybrid **6N** (9.8 mg, 0.015 mmol) and [RhCl(CO)₂]₂ (2.9 mg, 0.0075 mmol) were placed in a Schlenk flask, which was then degassed and purged with N₂ repeatedly. A mixture of acetophenone (350 mL, 3.0 mmol), diphenylsilane (840 mL, 4.5 mmol), and THF (4.5 mL) was added to the flask, and the resulting mixture was stirred at room temperature. The consumption of the ketone was monitored by TLC. After 6 h, the reaction mixture was hydrolyzed (3% HCl/MeOH), and the yield of 1-phenylethanol was determined by ¹H NMR (91%). When the hybrid **6S** was used in place of **6N**, the ketone was consumed within 30 min to afford the alcohol in 87% yield.

Hydrosilylation of Phenylacetylene Using 6X/[RhCl(CO)₂]₂. The hybrid **6X** (0.010 mmol) and [RhCl(CO)₂]₂ (1.9 mg, 0.0050 mmol) were placed in a Schlenk flask, which was then degassed and purged with N₂ repeatedly. A mixture of phenylacetylene (110 mL, 1.0 mmol), dimethylphenylsilane (230 mL, 1.5 mmol), and THF (1.5 mL) was added to the flask, and the resulting mixture was stirred at room temperature. The progress of the reaction was monitored by TLC. After 24 h, the acetylene was consumed completely, and the reaction mixture was analyzed by ¹H NMR spectroscopy. The three reaction products, β -Z-, β -E-, and α -styrenes, were characterized by comparison with authentic specimen. The yields and relative ratios are listed in eq 3.

Acknowledgment. This work was supported by a Grant-in-Aid (No. 19027030) from the Ministry of Education, Culture, Sports, Science, and Technology of Japan. We thank Prof. Hidemitsu Uno (Ehime University) for his helpful suggestions about X-ray crystallographic analysis. T.N. thanks a JSPS fellowship for young scientists.

Supporting Information Available: Experimental details, synthetic procedures, and characterization data for newly prepared compounds, ¹H NMR charts for new compounds, CIF files for **5O**, **6N**, **7O**, **10**, **11**, and **13S**, and complete ref 53 (ref 5 in Supporting Information). This material is available free of charge via the Internet at <http://pubs.acs.org>.

JA076709O

- (57) Sheldrick, G. M. *SHELXS-97/SHELXL-97*; University of Göttingen: Germany, 1997.
- (58) PATTY: Beurskens, P. T.; Admiraal, G.; Beurskens, G.; Bosman, W. P.; Garcia-Granda, S.; Gould, R. O.; Smit, J. M. M.; Smykalla, C. The DIRDIF program system. Technical Report of the Crystallography Laboratory; University of Nijmegen: Nijmegen, The Netherlands, 1992.
- (59) DIRDIF99: Beurskens, P. T.; Admiraal, G.; Beurskens, G.; Bosman, W. P.; deGelder, R.; Israel, R.; Smits, J. M. M. The DIRDIF program system. Technical Report of the Crystallography Laboratory; University of Nijmegen, Nijmegen, The Netherlands, 1999.
- (60) *CrystalStructure 3.8.0: Crystal Structure Analysis Package*; Rigaku and Rigaku/MSK: The Woodlands, TX, 2000–2006.